A "fracture testing" based approach to assess crack healing of concrete with and without crystalline admixtures

Liberato Ferrara [a,*], Visar Krelani [a], Maddalena Carsana [b]

[a] Department of Civil and Environmental Engineering, Politecnico di Milano, piazza Leonardo da Vinci 32, 20133 Milan, Italy
[b] Department of Chemistry, Material and Chemical Engineering, Politecnico di Milano, via Mancinelli 7, 20133 Milan, Italy

Received 13 November 2013
Received in revised form 10 June 2014
Accepted 3 July 2014
Available online 26 July 2014

1. Introduction

Worldwide increasing consciousness for sustainable use of natural resources has made "overcoming the apparent contradictory requirements of low cost and high performance a challenging task" [1] as well as a major concern. The importance of sustainability as a requisite which has to inform structure concept and design has been also recently highlighted in Model Code 2010. In this context, the availability of self-healing technologies, by controlling and repairing "early-stage cracks in concrete structures, where possible", could, on the one, hand prevent "permeation of driving factors for deterioration", thus extending the structure service life, and, on the other hand, even provide partial recovery of engineering properties relevant to the application [1,2].

As pointed out by Lauer and Slate already in 1956 [3] "if the mechanism of the action is understood, and means can be found for accelerating it, a great stride will have been made in effectively retarding" the rate of degradation of concrete and corrosion of embedded steel reinforcement, which are among the major problems of the concrete durability [4].

Discovered as early as in 1836 by the French Academy of Science, and attributed to the transformation of calcium hydroxide ($Ca(OH)_2$) into calcium carbonate ($CaCO_3$) as a consequence of exposure to the carbon dioxide (CO_2) in the atmosphere, autogeneous healing of concrete was also later observed by Abrams [5], who attributed it to the "hydraulicity" of residual un-hydrated cement, as well as by Loving [6], who, on inspection of concrete pipe culverts, found many healed cracks filled with calcium carbonate.

As a matter of fact, besides the availability of CO_2 in the exposure environment, the age of concrete at the time of cracking also governs the mechanism with the highest autogenous healing

* Corresponding author.
E-mail address: liberato.ferrara@polimi.it (L. Ferrara).

Table 1
Mix composition of investigated concretes (dosages in kg/m^3).

Constituent	Without additive	With additive
Cement type II 42.5	300	300
Water	190	190
Superplasticizer (lt/m^3)	3	3
Fine aggregate 0–4 mm	1078	1080
Coarse aggregate 4–16 mm	880	880
Crystalline additive	=	3

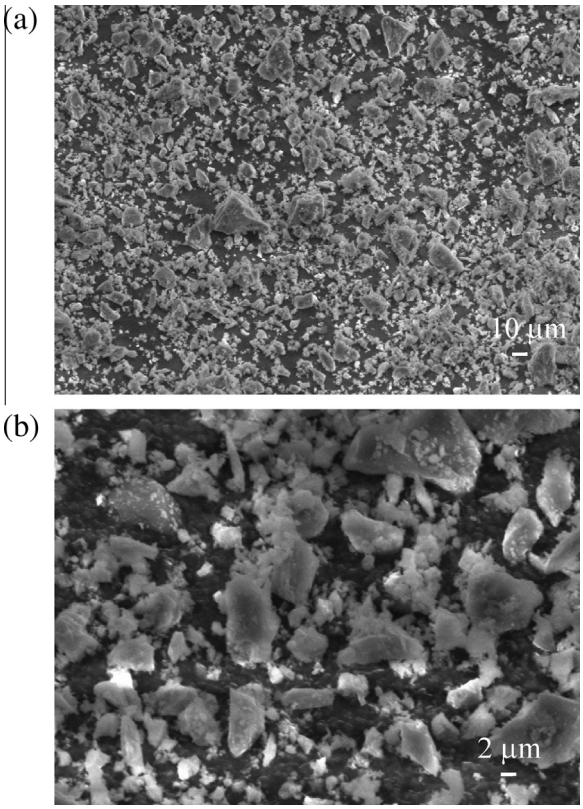

Fig. 1. SEM images of a powder sample of crystalline additive observed at different magnifications (a) e (b).

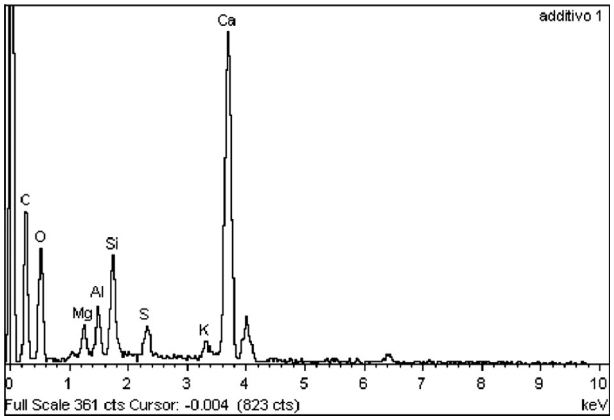

Fig. 2. EDS analysis of the additive particles shown in Fig. 1.

capacity. Due to its relatively high content of unhydrated cement particles, ongoing/delayed hydration is the main healing mechanism in young concrete [7–9], whereas at a later age, calcium carbonate precipitation becomes the major one.

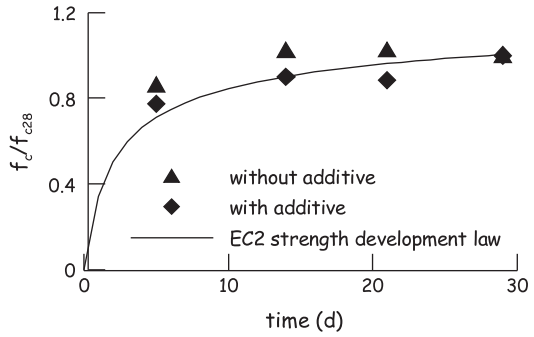

Fig. 3. Strength development of concrete with and without crystalline additives vs. EC2 provisions (fc28 = 29.9 N/mm^2 and 27.4 N/mm^2 for concrete without and with the crystalline additive respectively – each data point average of two nominally identical tests).

The action of autogeneous healing may have "practical value in several applications (...) namely: (...) repair of precast units cracked during early handling; sealing against corrosion and re-knitting of cracks developed in concrete piles during their handling and driving; sealing of cracks in concrete water tanks; and the regain, after loss, of strength of "green" concrete disturbed by vibrations" [10]. Further evidence of the effects of crack healing on the recovery of mechanical properties was reported by Whitehurst [11], who observed an increase in the dynamic modulus of field structures during a wet spring, following a winter of freezing and thawing. Anyway, whereas significant reduction in water permeability was observed because of crack healing [12–14], reported recovery of mechanical properties [3,14,15] was not so spectacular. With reference to the maximum crack width that can be healed without any external intervention, a wide range of openings has been reported by different authors (i.e. from as low as 5 to as high as 300 µm) [16–18].

Consensus among the international community has been achieved about the engineering significance of the problem, which has resulted in state-of-the-art reports to be compiled as well as into a clear terminology definition. The RILEM TC-221-SHC "Self-healing phenomena in cement based materials" [1], distinguishes:

- based on the result of the action, between self-closing and self-healing, whether only closure of the cracks or also restoring of the mechanical properties is observed;
- based on the process of the action, between "autogenic" (or natural) and "autonomic" (or engineered) self closing/healing, whether the crack closure or restoration of material properties is due to either the concrete material itself or some engineered addition.

In the very last decade a huge amount of research work has been dedicated to "engineered" self-healing, along different main directions of investigation: self healing engineered with fibre reinforcement [20–28], mineral-producing bacteria [29], super absorbent polymers [30], healing agents contained in shell and tubular capsules [31,32] and other proprietary chemical admixtures [33], such as alumino-silicate materials and various modified calcium composite materials. In the latter case, the self-healing action is mainly due to the filling of the crack width, swelling and expansion effects and to improved hydration and re-crystallization. The supply of water (moisture) is essential, especially in the case of addition of chemical agents able to promote the deposition of crystals inside the crack, but "since most infrastructures are exposed to rain or underground water, usually this is an easily satisfiable requirement" [33].

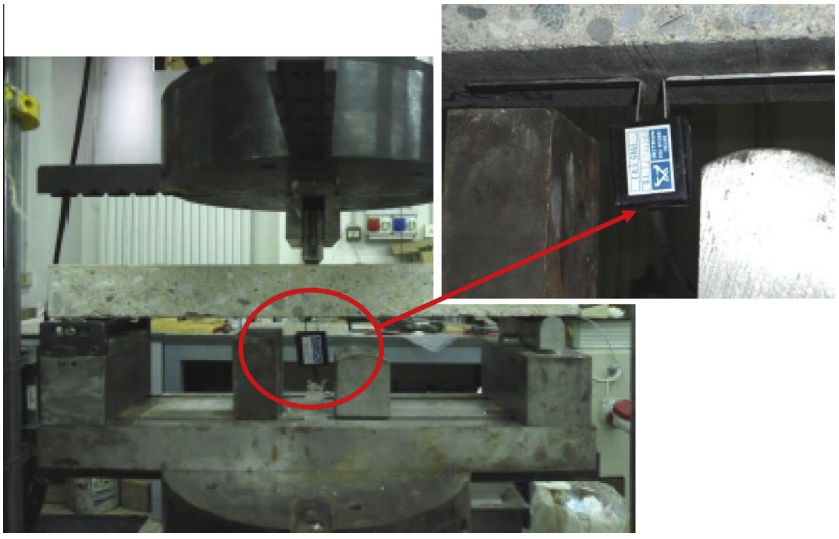

Fig. 4. 3-Point bending test set-up for specimen pre-cracking (beam span = 450 mm).

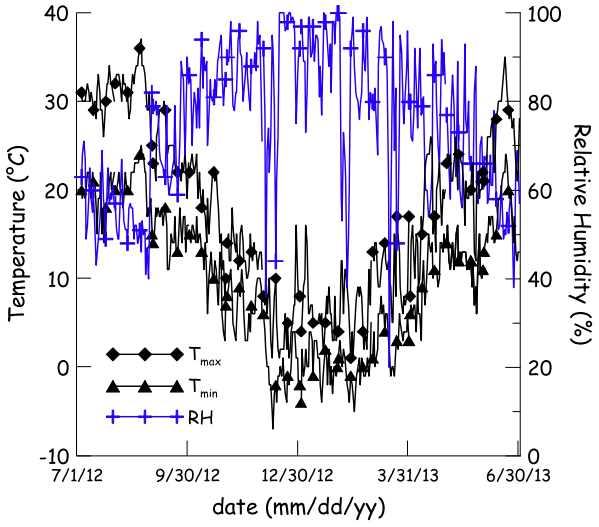

Fig. 5a. Temperature and relative Humidity recorded along the exposure period.

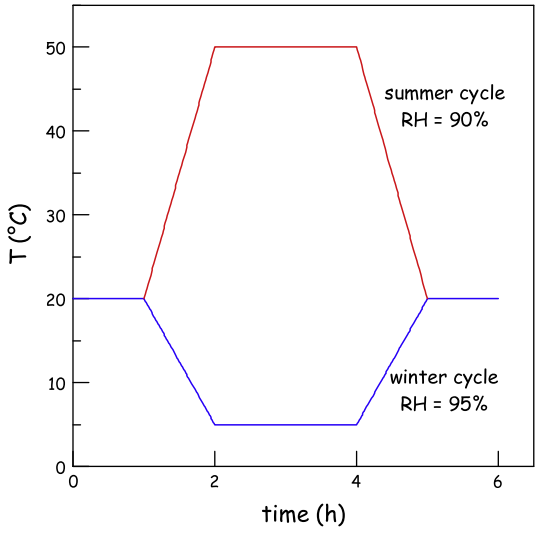

Fig. 5b. Temperature and relative Humidity cycles for climate chamber conditioning.

Besides the presence of water, several other variables can affect the phenomenon of self healing, such as the mix proportions [15], the stress state along the cracks and the steadiness of the cracked state [19] as well as thermal and hygrometric conditions [3,16].

Moreover, traditional mineral additions for cement replacement, such as fly ash or blast furnace slag [34,35], or even innovative pozzolanic additions [36,37], investigated by different researchers, may also promote autogeneous healing because of delayed hydration, since high amounts of these binders remain un-hydrated even at a later age because of the slow pozzolanic reactions or, as in the case of slag, because of latent hydraulicity.

Among the aforementioned proprietary chemical admixtures, the so-called "crystalline additives", containing substances which react with cement constituents and form calcium silicate hydrates and already employed for the reduction of concrete porosity and of water permeability of concrete, can effectively serve also as self healing engineering additions [26].

The "crystallization" reactions, which propagate completely through the concrete mass resulting in a system impervious to water and other environment born aggressive substances, consume the moisture inside the concrete but can also undergo a delayed activation, whenever the material comes back into contact with water and/or environment moisture: this, as a matter of fact, can happen upon crack formation even at later ages.

In this paper an experimental methodology is proposed to evaluate the effects of crack healing on the mechanical properties of concrete, with reference to both autogenic self-healing and engineered through the addition of a crystalline admixture. The crystalline admixture employed in this study, which will be described in the forthcoming section, consists of a mix of cement, sand and active silica and is added to the raw concrete constituents before mixing.

The proposed methodology, which will also be described in detail in the forthcoming section, is based on 3-point bending tests performed up to controlled crack opening and up to failure, respectively before and after exposure/conditioning. Different exposure conditions have been considered, namely immersion in water immersion, exposure to open air and accelerated temperature cycles.

Table 2
Synopsis of experimental programme (n° of specimens per each test condition).

	Exposure condition and duration															
	Water immersion					Open air exposure					Climate chamber					
											Winter			Summer		
	1m	2m	3m	6m	12m	1m	2m	3m	6m	12m	1w	2w	4w	1w	2w	4w
w/out additive																
uncracked	1	2	2	2	2	1	2	2	2	2	2	2	2	3	3	3
Precracked 100 μm											2	2	3	3	3	3
Precracked 200 μm	1	2	2	2	2	1	2	2	2	2	3	3	3	3	3	3
With additive																
Uncracked	1	2	2	2	2	1	2	2	2	2	2	2	2	6	6	6
Precracked 100 μm											2	2	3	6	6	6
Precracked 200 μm	1	2	2	2	2	1	2	2	2	2	3	3	3	6	6	6

m = months.
w = weeks.

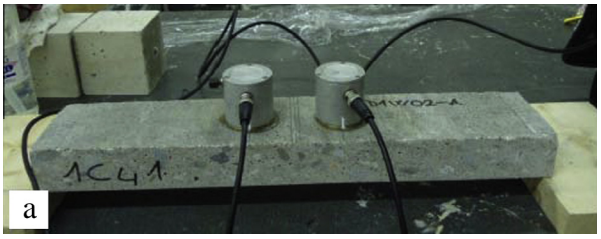

Fig. 6. Set-up for Ultrasonic Pulse Velocity tests: distance between the emitter and receiver: 90 mm – diameter of the sensors: 50 mm – employed signal frequency: 50 kHz).

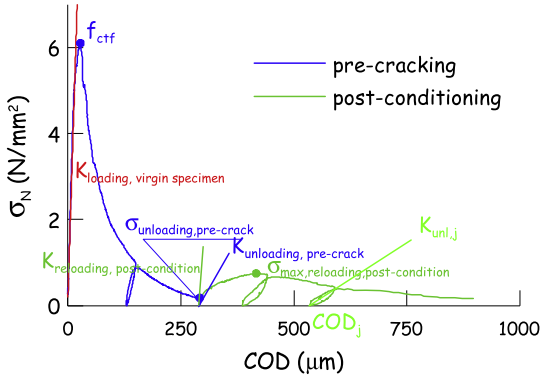

Fig. 7. Example of stress vs. COD curves for specimens submitted to pre-cracking and post-conditioning 3pb tests; definition of quantities for calculation of self healing indices.

The effects of the self-healing of cracks on the recovery of stiffness and load-bearing capacity have been evaluated, also with the aid of Ultrasonic Pulse Velocity (UPV) tests, optical microscopy observations and Scanning Electron Microscope (SEM) analyses at selected "crack healed" locations. The results thus garnered were instrumental in defining and quantifying self-healing related indices, which could be implemented into a durability based design framework, as currently addressed by international design codes.

2. Experimental methodology

The mix composition of the normal strength concrete employed in this study is detailed in Table 1. Because of the interest to evaluate the effects of crystalline additives on the self healing capacity of concrete, a companion mix has been also produced with a 1% additive addition, by weight of cement (Table 1). The additive was dry mixed with the raw aggregates, at the very beginning of the mixing sequence, which was then followed by addition of cement and, upon further mixing, by the incorporation of water and superplasticizer.

The particles of the employed crystalline admixture are shown in Fig. 1. They have irregular shape and size in the range of about 1–20 μm; their morphology is similar to that of cement grains. The EDS microanalysis in Fig. 2 highlights the presence of calcium, oxygen, silicon, magnesium, aluminium and potassium. This spectrum is comparable with that of an Ordinary Portland Cement (OPC), except for the peak of sulphur which is slightly higher.

Slabs 1 m long × 0.5 m wide and 50 mm thick were casted with both concretes with and without the additive; after three days curing in fog room at 20 °C temperature and 95% Relative Humidity (RH) and under wet towels, slabs were cut into prismatic "beam-like" specimens, each 500 mm long and about 100 mm wide. Specimens were cured in the same fog room, for a period ranging between 35 and 42 days. Along the curing period the development of strength was monitored, for both concrete mixes, by means of compressive strength tests on 150 mm cube companion specimens. Results plotted in Fig. 3 clearly show that the addition of crystalline admixtures had scant effect on the strength development.

In order to evaluate the self healing capacity of concrete and its effects on the recovery of mechanical properties, at the end of the aforementioned curing period, the beam specimens were pre-cracked, up to different levels of residual crack opening, equal to about 100 and 200 μm. Specimens were pre-cracked employing the three-point bending (3pb) test set-up shown in Fig. 4: the tests were performed using the Crack Opening Displacement (COD) at mid-span as a control variable. Some specimens were kept un-cracked for reference as well. All the specimens were then subjected to different controlled exposure conditions:

- immersion in water at constant temperature, equal to 20 °C, up to 1 year;
- exposure to air, up to 1 year, while daily recording minimum and maximum temperature and average RH, whose trends are plotted in Fig. 5a;
- exposure in climate chamber to temperature cycles, representative of typical either winter or summer daily excursions in Northern Italy. The cycles are shown in Fig. 5b; exposures up to 4 weeks for each type of cycle has been scheduled.

Table 2 provides a synoptic view of the experimental programme as a whole.

At the end of the scheduled exposure times, 3pb tests were performed again on each and all the specimens up to complete failure (it is worth remarking that all specimens were, in case, wiped and allowed for a couple of hours to condition at 20 °C and 65% RH before final tests). The nominal bending stress vs. COD response exhibited by the same specimen in its virgin state, i.e. when undergoing the pre-cracking stage test, and at the end of the prescribed exposure condition and duration in the cracked state were compared. The recovery, if any, of stiffness and load bearing capacity, as attributable to crack healing phenomena, will be thus evaluated, as it will be detailed in the forthcoming section This was instrumental at defining and quantifying suitable self healing indices for the analysed mechanical properties.

Ultrasonic Pulse Velocity (UPV) tests were performed employing the set-up shown in Fig. 6, in which details of the test set-up are also given; UPV tests were performed: on the virgin specimen, after the pre-cracking and before the onset of the conditioning and, finally, before final fracture tests at the end of the scheduled conditioned periods.

At the end of final fracture tests observation on fracture surfaces of selected specimens were performed by using an environmental scanning electron microscopy ZeissEvo 50P equipped with oxford Inca Energy 200EDS having a ultra-thin window detector from 133 eV.

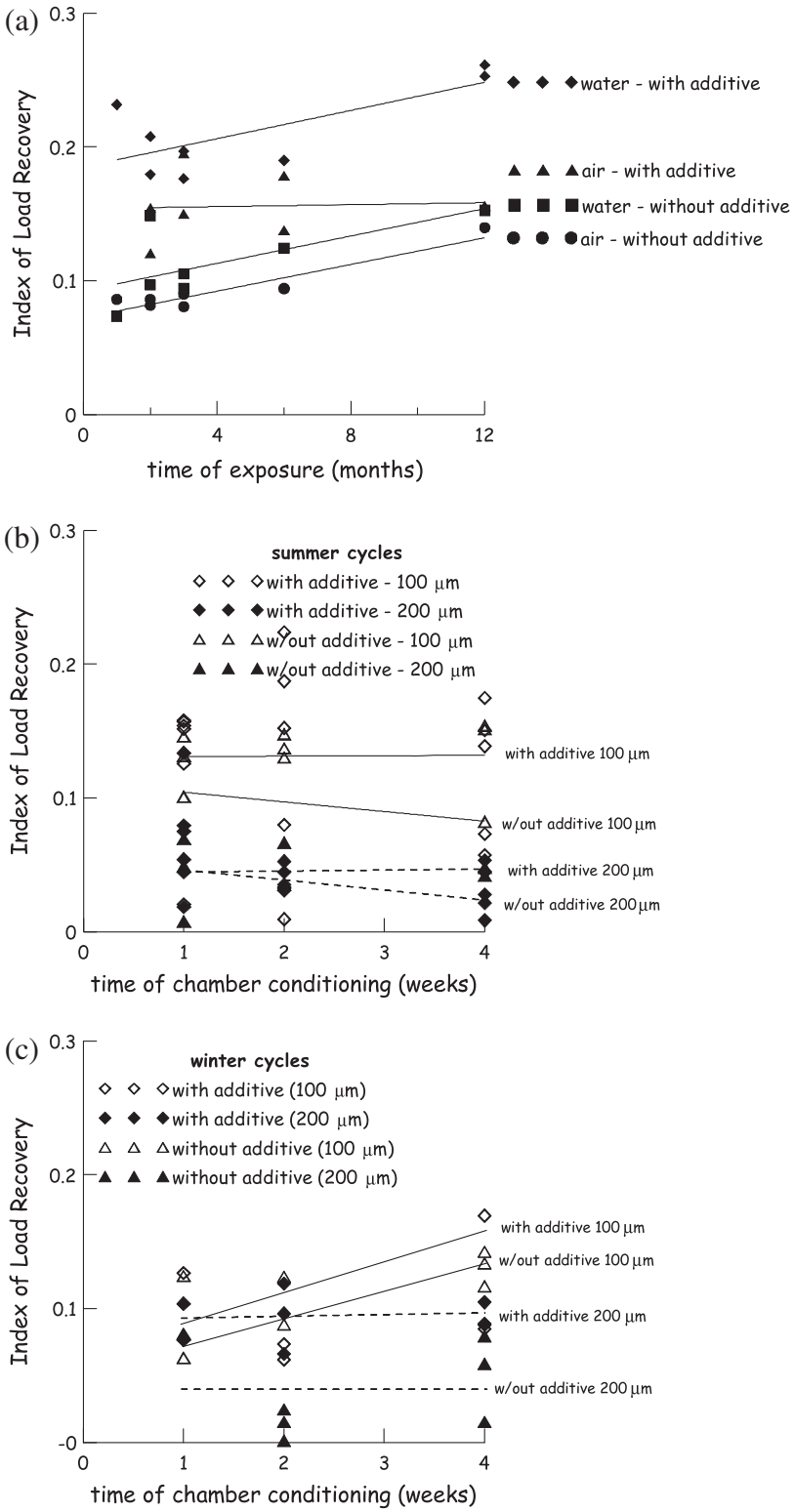

Fig. 8. Index of Load Recovery (as evaluated from 3pb test results) vs. exposure time for water immersion/air exposure (a); summer (b) and winter (c) chamber conditioning.

3. Experimental results: analysis and discussion

3.1. Three-point bending tests

In Fig. 7 the results of a typical test are shown, in terms of nominal stress σ_N vs. COD curves: it is worth remarking that the graphs are built up in such a way that the curves pertaining respectively to the pre-cracking test and to the post-conditioning failure test performed on the same specimens are compared.

Data were analysed in order to define and calculate self healing indices as detailed hereafter:

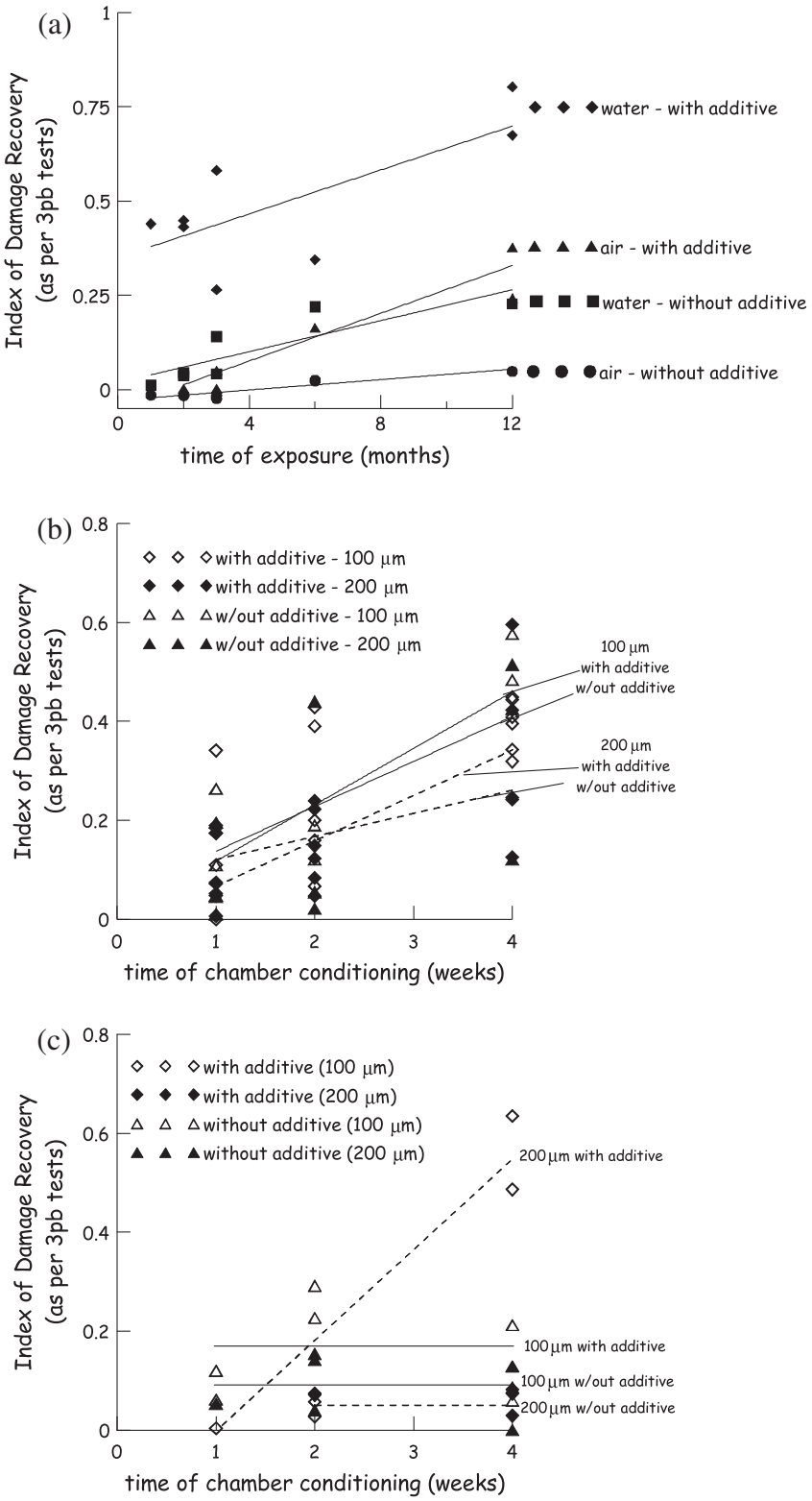

Fig. 9. Index of damage recovery (as evaluated from 3pb test results) vs. exposure time for water immersion/air exposure (a); summer (b) and winter (c) chamber conditioning.

3.1.1. Index of Load Recovery

From the values of nominal flexural strengths/stresses as denoted in Fig. 7 an Index of Load Recovery can be defined as:

$$\mathrm{ILR} = \frac{\sigma_{\mathrm{N,max\ reloading,\ \ post\text{-}conditioning}} - \sigma_{\mathrm{unloading,pre\text{-}crack}}}{f_{\mathrm{ctf}} - \sigma_{\mathrm{unloading,pre\text{-}crack}}} \quad (1)$$

Fig. 8a–c show the trend of the ILR, computed as above, vs. the exposure time.

3.1.2. Index of Damage Recovery as per 3pb tests

From values of flexural stiffness K evaluated at different stages of the fracture test protocol and as denoted in Fig. 7, an Index of Damage Recovery can be defined as:

$$IDR_{(3pb)} = \frac{K_{reloading,post\text{-}conditioning} - K_{unloading,pre\text{-}crack}}{K_{loading,virginspecimen} - K_{unloading,pre\text{-}crack}} \quad (2)$$

Fig. 9a–c show the trend of the IDR, computed as above, vs. the exposure time.

Cross analysis of graphs in Figs. 8 and 9 allows the following remarks to be highlighted:

– specimens immersed in water showed, since from the beginning, some load recovery capacity, which was higher for specimens

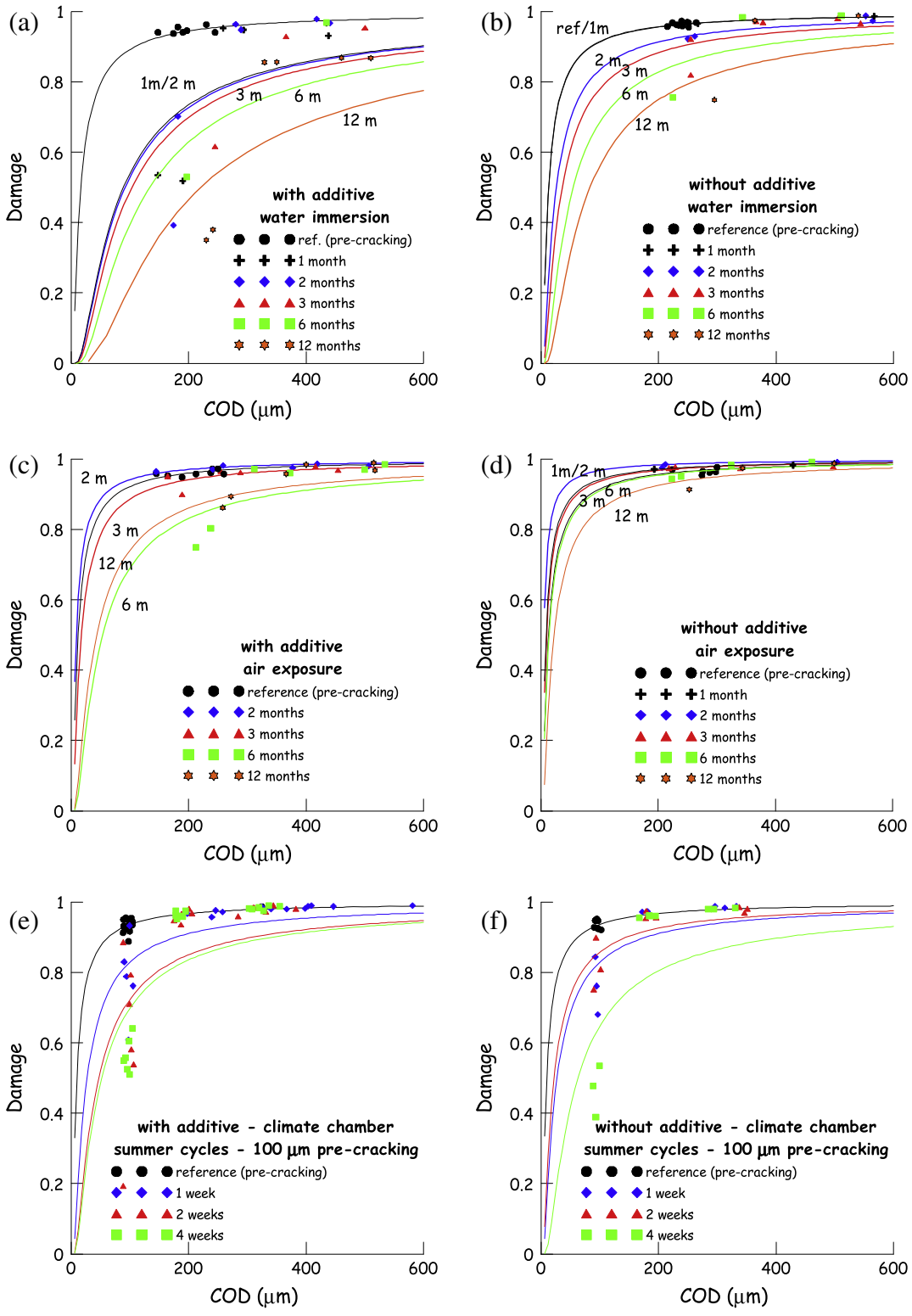

Fig. 10. Fitted damage evolution laws for precracked concrete specimens with (a, c, e, g, i, k) and without (b, d, f, h, j, l) crystalline additive and different exposure conditions: water immersion (a, b); air exposure (c, d); climate chamber conditioning in summer climate (e–h) for specimens pre-cracked at 100 μm (e, f) and 200 μm (g, h); climate chamber conditioning in winter climate (i–l) for specimens pre-cracked at 100 μm (i, j) and 200 μm (k, l).

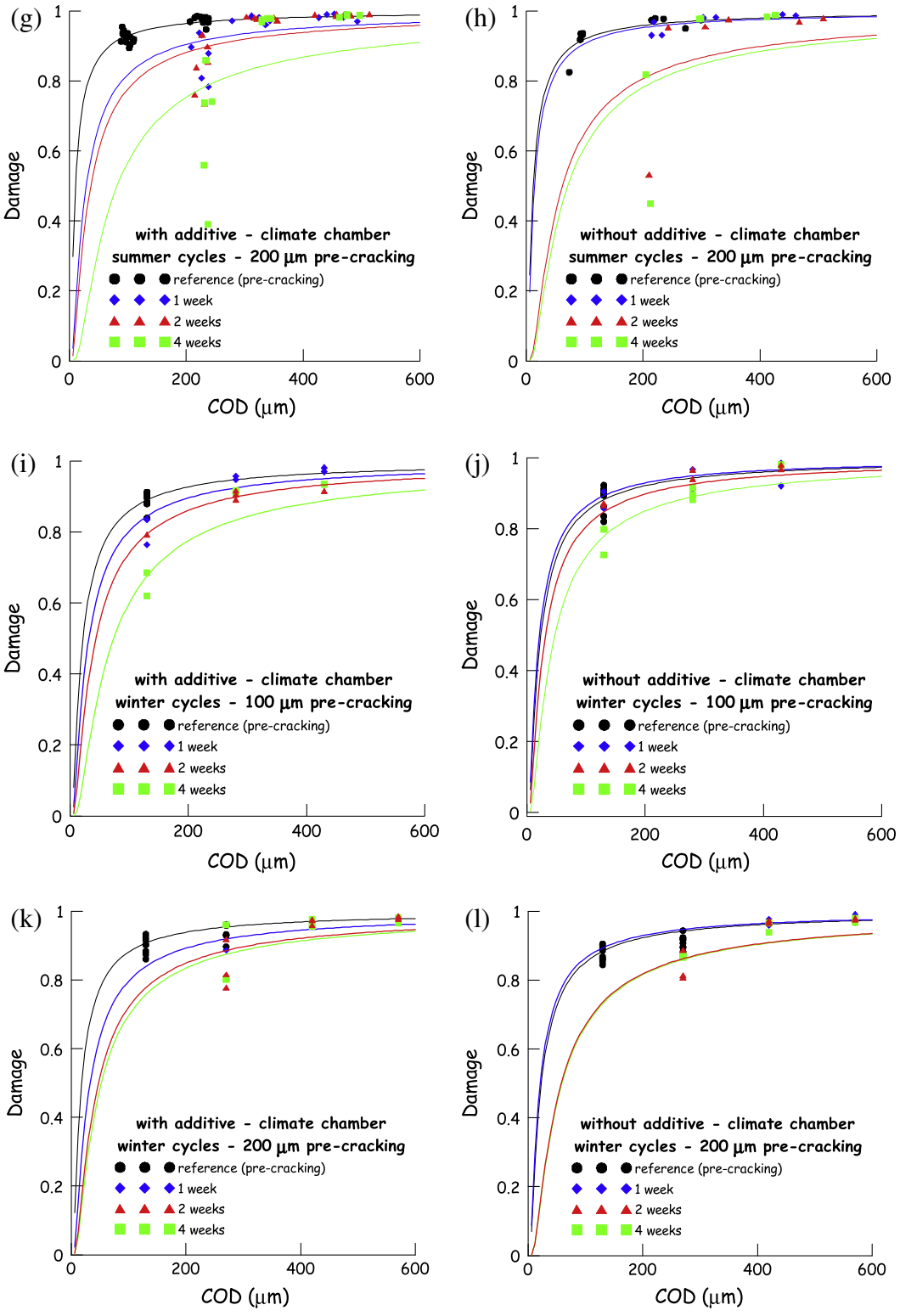

Fig. 10 (*continued*)

containing the crystalline additive, and continued to moderately increase with immersion time, with similar trend for specimens with and without the additive; the maximum attained level of load recovery was not higher than 25% of the softening stress decay experienced upon pre-cracking;

– specimens exposed to air and containing the additive showed an initial load recovery capacity lower than specimens with the additive immersed in water but higher than all specimens without the additive; this confirms that additive particles, because of their hydrophilic nature, can capture air moisture and react with it promoting self healing; nonetheless, the recovery did not exhibit significant changes upon prolonged exposure, as a combined effect of the consumption of the available crystalline additive and of the moisture

available in the air, as also affected by daily and seasonal fluctuations;
- specimens exposed to air and without the crystalline additive showed, as expected, the lowest performance in terms of load recovery capacity due to self healing, even with a moderately increasing trend, as resulting from the available air moisture and the kinetic of delayed hydration of un-hydrated cement particles exposed upon cracking;
- in the case of climate chamber conditioning, results appear much more dispersed: in all cases, a lower recovery of the load bearing capacity was achieved, with respect to water immersion, for both winter and summer climates. Interestingly, whereas for winter cycles and lower crack openings, a continuous increase of the load recovery was observed, in all other cases results held constant, if not sometimes showed a worsening trend, as, e.g., for specimens without the additive exposed to summer cycles. This could be explained by a sort of drying effect caused by the higher attained temperatures, which may exacerbate the already existing damage (cracks), and which the presence of crystalline additives were able to counteract to some extent. Anyway no definite conclusion can be drawn because of the high dispersion of results.

3.1.2.1. Damage evolution laws. As shown by the example nominal stress σ_N vs. COD curve in Fig. 7, all along the 3pb test loading path, both in the pre-cracking and post-conditioning stages, a series of unloading–reloading steps were performed. This allowed the values of secant unloading stiffness, $K_{unl,j}$, to be evaluated in correspondence of different values of the Crack Opening Displacement, COD_j, through which corresponding values could be calculated of a Continuum Damage variable, coherently meant as an index of stiffness degradation:

$$D(COD_j) = 1 - \frac{K_{unl,j}}{K_{loading,virginspecimen}} \quad (3)$$

with notation once again explained in Fig. 7.

It was thus possible to build up the evolution laws of the damage variable vs. COD, through an exponential fitting of the data as:

$$D(COD) = \exp[-A/COD] \quad (4)$$

where A is a fitting constant, correlated to the speed of damage accumulation with progressive crack opening: the higher A, the slower the damage growth.

Damage evolution laws built as above are shown in Fig. 10a–n for all the investigated cases. The following statements hold, which are also in agreement with the previously shown trends of the indices of both load and damage recovery:

- specimens with the additive immersed in water (Fig. 10a) exhibited the largest effects in terms of "slowering" of the damage evolution law along the exposure time;
- for specimens without the additive immersed in water (Fig. 10b) an almost constant trend in the diminution of the damage evolution law has been observed as a result of the healing phenomena due to continued hydration; anyway these effects appear only after two months exposure, unlikely than in the previous case; as a whole the recovery of the performance is lower than in the case with the additive;
- effects of healing in specimens containing the additive and exposed to air (Fig. 10c) are initially slow, as witnessed by the closeness of the damage curves for conditioned specimens to that calibrated on the virgin ones; only after six months exposure some recovery appears, which does not seem to proceed further upon prolonged exposure;
- specimens not containing the additive and exposed to air (Fig. 10d) show the poorest recovery all along the investigated exposure period;
- specimens exposed to environmental summer and winter climate chamber conditioning (Fig. 10e–l) show a gradual recovery of performance both in the case with (Fig. 10e, g, i, k) and without the additive (Fig. 10f, h, j, l); recovery is, at least initially, faster, as expectable, in the former case; anyway the large dispersion of results, already detected with reference to the index of damage recovery, may to some extent undermine the true representativeness of the plotted damage trends, which can hence be taken as only qualitatively significant.

3.1.3. Indices of crack healing

From the nominal bending stress σ_N vs. COD curves as well as from the damage vs. COD evolution laws, an estimation of the crack closure due to the self healing can be provided.

3.1.3.1. Crack healing from σ_N–COD curves. The proposed methodology (Fig. 11a) consists in operating a "backward" shifting along the COD axis, of the stress–COD curve representative of the behaviour of each pre-cracked specimen after environment conditioning, until the stress–COD curve of the same specimen, as measured during the pre-cracking test on the virgin undamaged sample is met. The new value of the "origin" COD can be estimated by drawing, from the aforementioned point on the curve of the virgin sample, an unloading branch with a slope equal to that of the closest unloading previously measured on the virgin sample itself. This

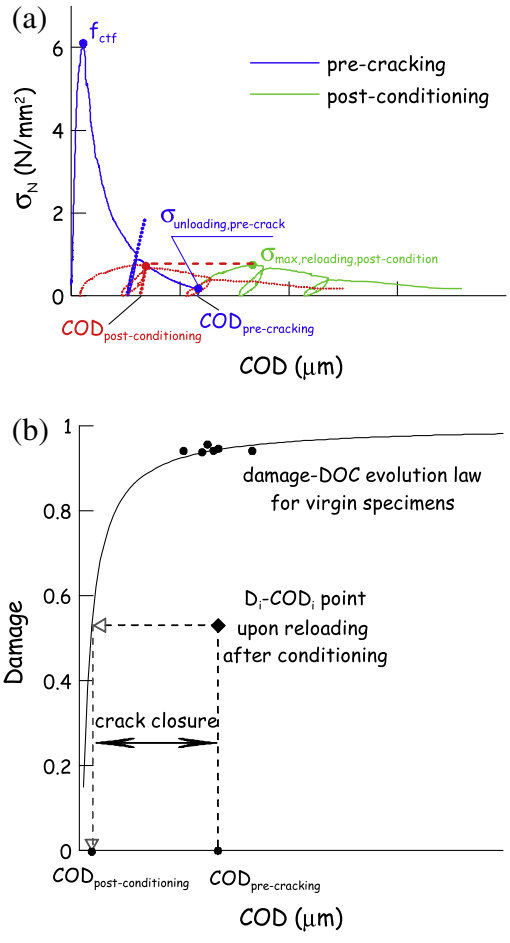

Fig. 11. Graphical explanation of the procedure to estimate crack closure from σ_N–COD curves (a) and from D-COD evolution laws built as in Fig. 10a–n.

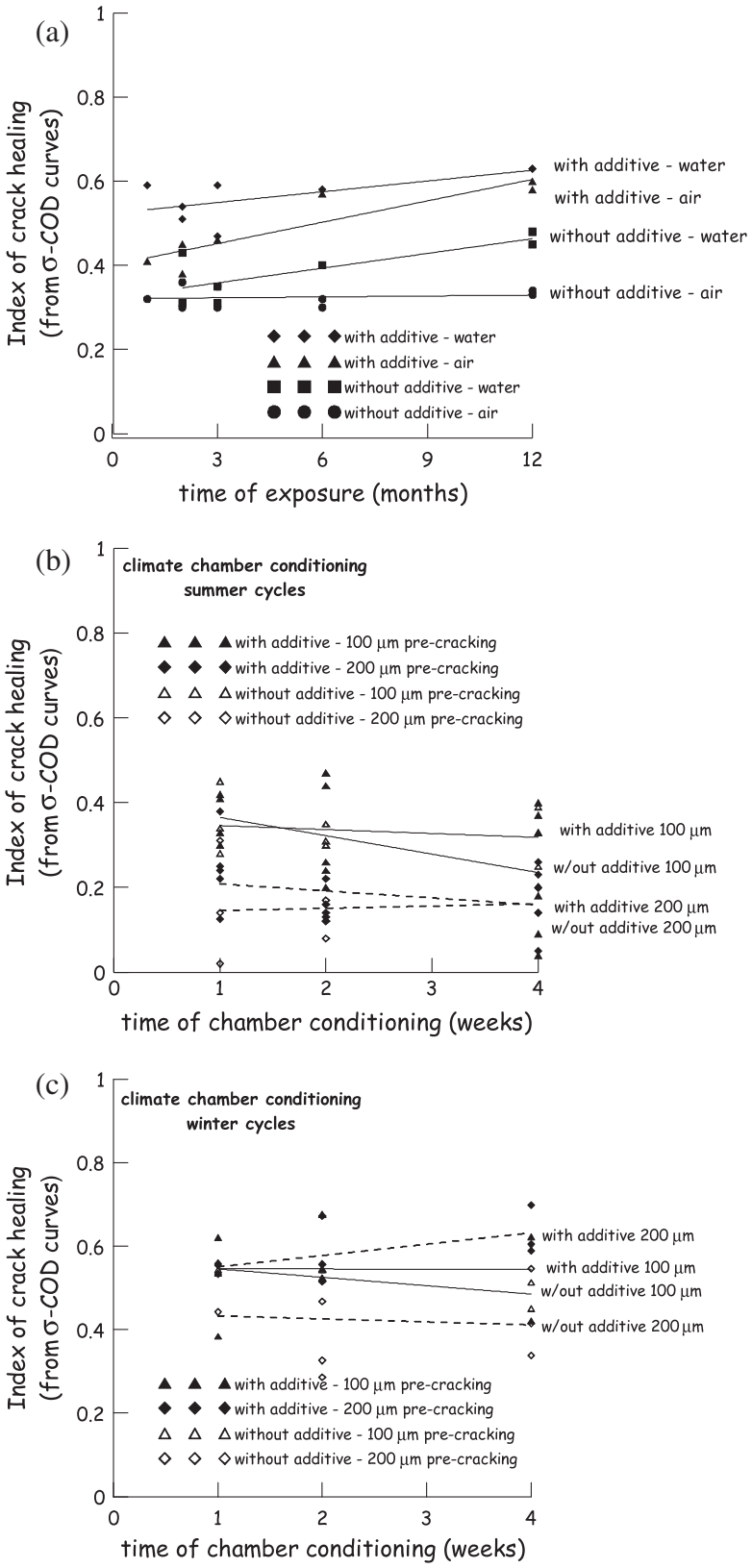

Fig. 12. Index of Crack Healing (as evaluated from σ–COD curves) vs. exposure time for water immersion/air exposure (a); summer (b) and winter (c) chamber conditioning.

allows to define and quantify an index of crack healing as in Eq. (5), whose trends are shown in Fig. 12a–c:

$$\mathrm{ICH}_{\text{stress-crack opening}} = \frac{\mathrm{COD}_{\text{pre-cracking}} - \mathrm{COD}_{\text{post-conditioning}}}{\mathrm{COD}_{\text{pre-cracking}}} \quad (5)$$

3.1.3.2. Crack healing from D-COD evolution laws. The proposed methodology (Fig. 11b) consists first of all in identifying the points representative of damage-COD, as evaluated upon reloading the specimen after environmental conditioning, assuming the initial crack opening coincided with the value measured at unloading

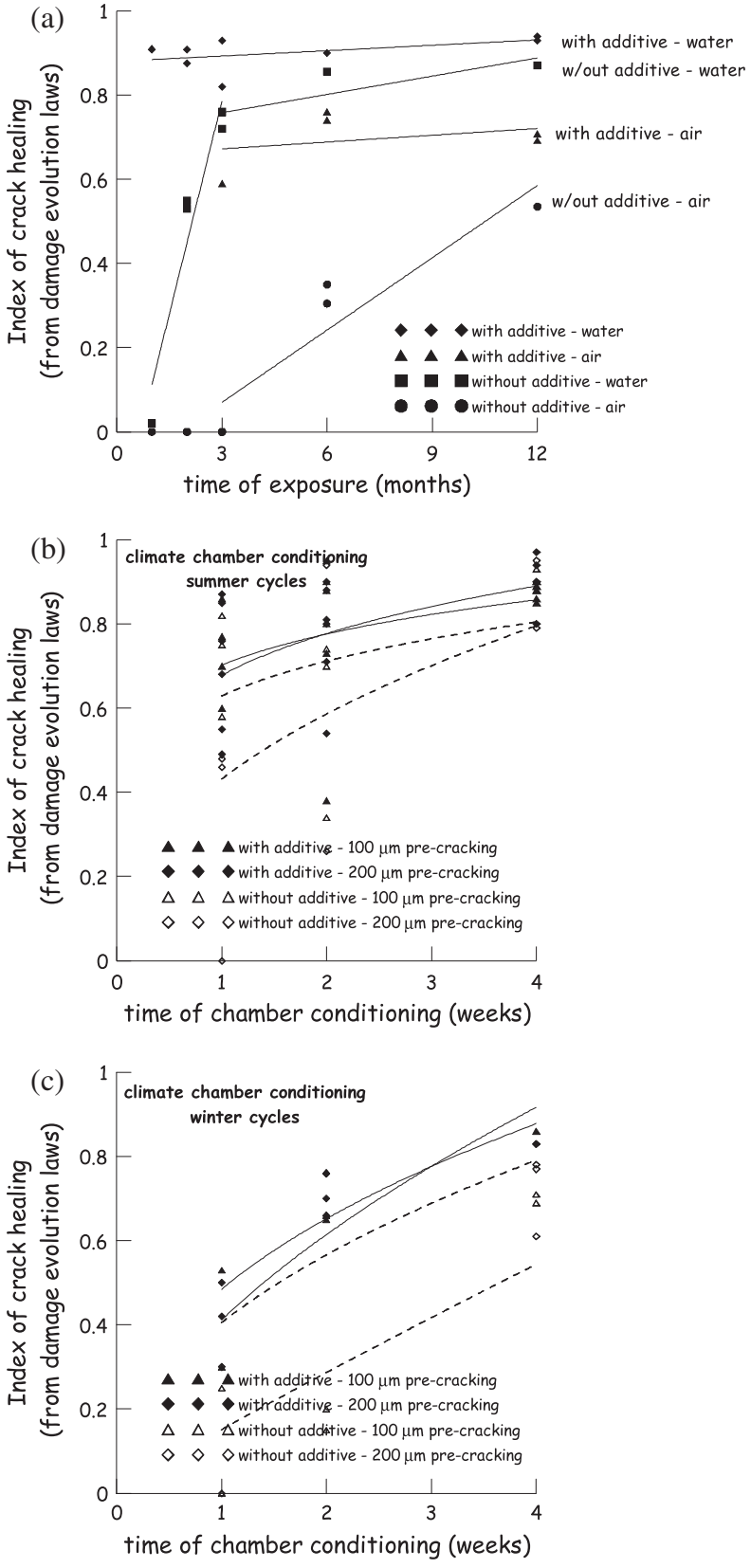

Fig. 13. Index of Crack Healing (as evaluated from damage evolution laws) vs. exposure time for water immersion/air exposure (a); summer (b) and winter (c) chamber conditioning.

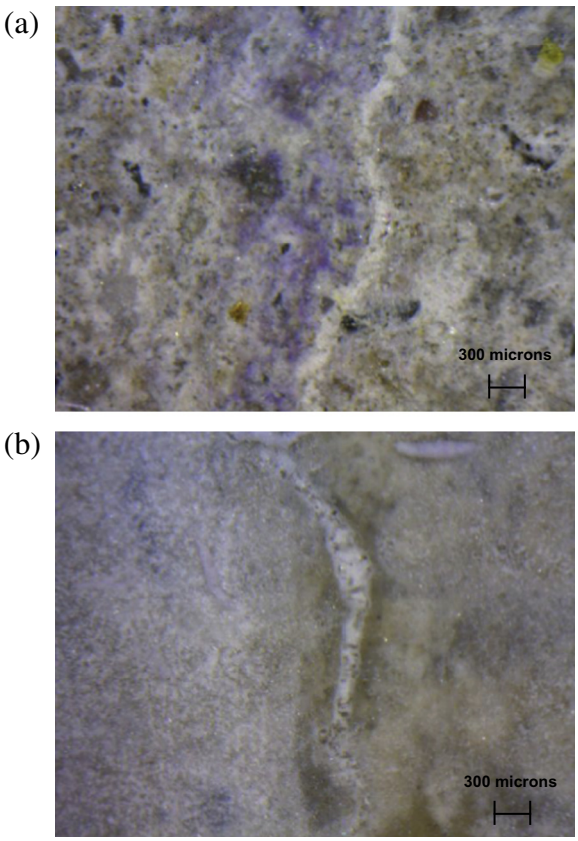

Fig. 14. Healed cracks for specimens with (a) and without (b) crystalline additive after six months of immersion in water.

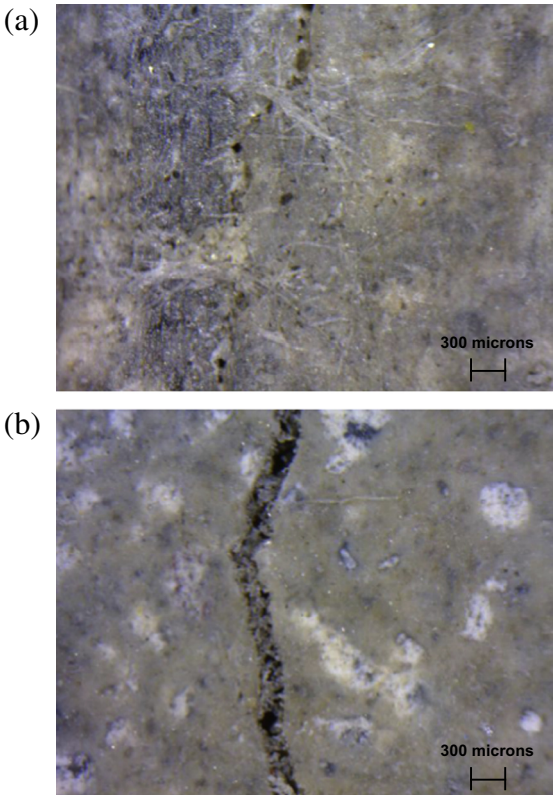

Fig. 15. Healed/healing cracks for specimens with (a) and without (b) crystalline additive after six months of exposure to open air.

during the pre-cracking stage. The points, identified as above, are then "shifted backward" along the COD axis until the fitted damage-COD evolution curve of the virgin specimen is met: the amount of this backward shifting can be assumed as an indicator of the crack closure effect produced by the self healing phenomena. The related index of crack healing is thus defined as in Eq. (6), whose trend are plotted in Fig. 13a–c.

$$\mathrm{ICH}_{\text{damage evolution}} = \frac{\mathrm{COD}_{\text{pre-cracking}} - \mathrm{COD}_{\text{post-conditioning}}}{\mathrm{COD}_{\text{pre-cracking}}} \tag{6}$$

The cross analysis of data shown in Figs. 12a–c and 13a–c, despite quantitative differences, (indices estimated from damage evolution laws are somewhat higher than those estimated from σ_N–COD curves), allows the following remarks to be highlighted:

- a remarkable crack closure may occur, since from the beginning of the surveyed exposure times, for specimens containing the crystalline additive and immersed in water; the same specimens, when exposed to air, show a slower recovery capacity;
- immersion in water triggers the self healing also for specimens without any additive, but at a much slower pace: only after 2–3 months effects start being visible and after 6 months a performance comparable to specimens with the additive was achieved; specimens without any additive exposed to air hardly show any appreciable recovery and only after prolonged exposure a moderate crack closure starts appearing;
- in the case of climate chamber conditioning, for both the summer and winter cases, specimens with the additive show a better recovery, which is higher for tighter crack openings; The higher dispersion of results anyway, once again does not allow any quantitative firm conclusion to be drawn about the plotted trends.

Pictures obtained by stereo-microscope in Figs. 14–16 confirm the related findings.

3.1.4. Recovery of mechanical properties vs. crack healing indices

The trends of indices of recovery of mechanical properties vs. the related crack healing indices allow an insightful synopsis to be provided about the investigated phenomena as well as a preliminary methodological quantification to be attempted. Because of higher dispersion of results for climate chamber conditioned specimens, this analysis will be performed only on specimens immersed in water and/or exposed to air. Effects of exposure conditions and of the crystalline additive are evident. Moreover it can be highlighted that the trend of damage recovery vs. crack healing, estimated from damage evolution laws (Fig. 17a), coherently with the damage model assumptions, shows that a remarkable crack healing is needed in order to have an appreciable recovery of the specimen stiffness. Effects of crystalline additive in the concrete mix is also evident, from the higher levels of recovery of stiffness for equal healing of the cracks. On the other hand, the trend of the load recovery vs. crack healing (Fig. 17b) shows that some load bearing capacity is recovered even for very low values of estimated crack healing, with a more moderate influence of the additive, also considering the narrow data range provided by experiments. The captured trend is slower than the stiffness recovery one and hardly more than 20% of the stress decay experienced upon cracking could be garnered because of the crack healing. A better understanding could be achieved through a dedicated analysis of the strength development of crack healing products, as also affected by exposure conditions, which has been regarded as out of the scope of this work.

Comparison between the indices of crack healing, as evaluated both from σ_N–COD curves and from damage-COD fitted evolution laws is finally shown in Fig. 17c, always with reference to water

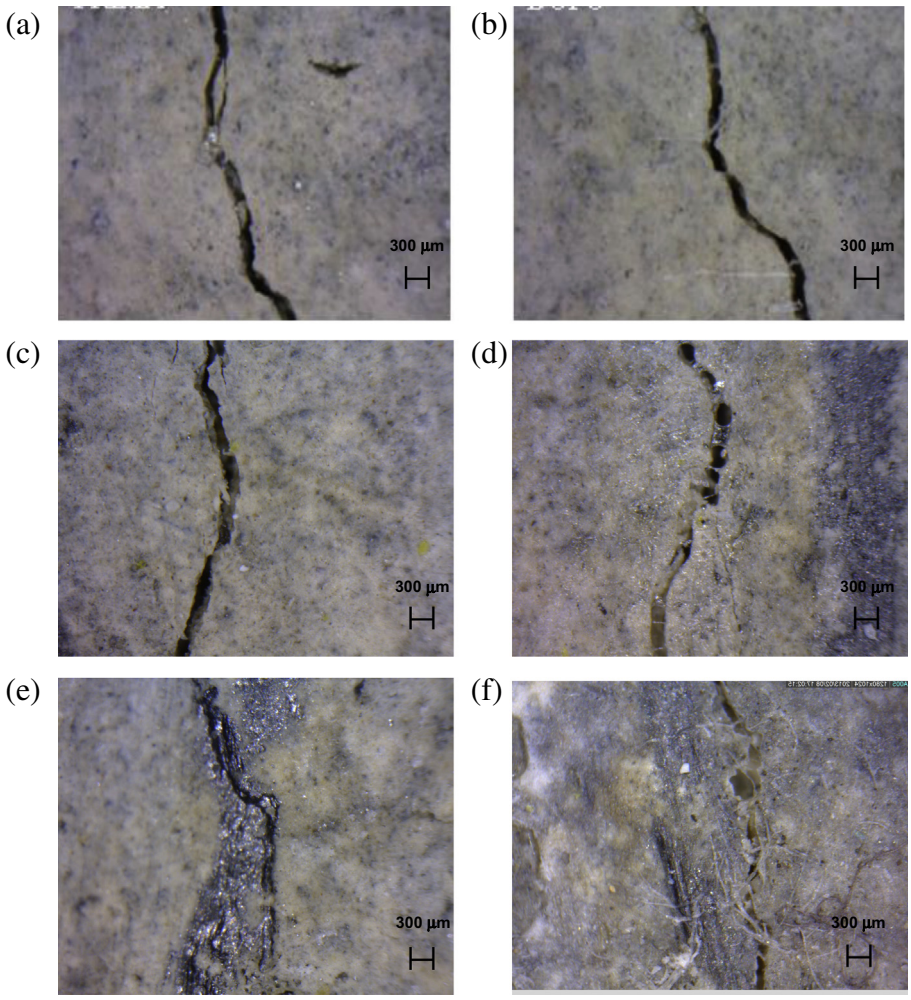

Fig. 16. Healing cracks for specimens with crystalline additive before exposure (a, c, e) and after one (b), two (d) or four weeks (f) in climate chamber (summer cycles).

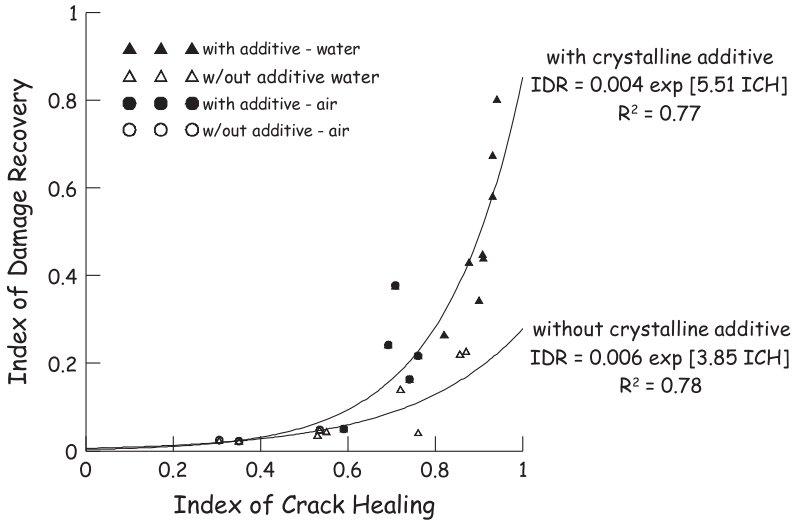

Fig. 17a. Index of damage recovery vs. index of crack healing as estimated from fitted damage evolution laws (see Fig. 11).

immersed and air exposed specimens only. Besides the quantitative trends (it looks that the lower load recovery capacity leads to a lower estimation of the crack healing), the more clear and reliable trend of the admixtures concrete significantly appears.

3.2. Ultrasonic Pulse Velocity tests

Wave speed was calculated from measured transit time between the emitter and receiver units of the UPV test apparatus,

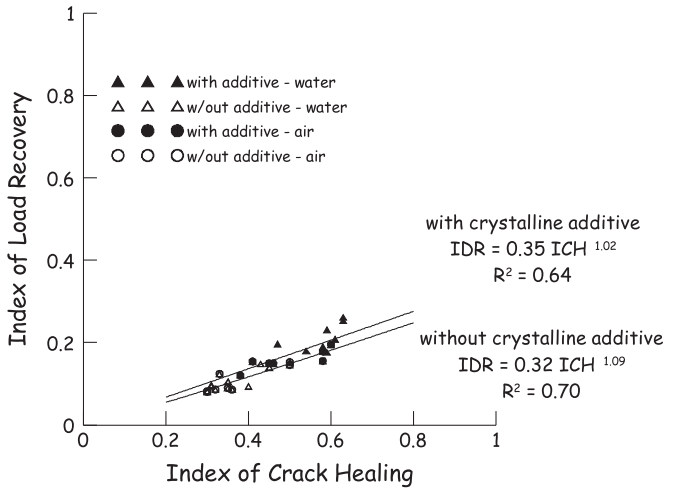

Fig. 17b. Index of Load Recovery vs. index of crack healing as evaluated from stress vs. COD curves obtained from 3pb tests.

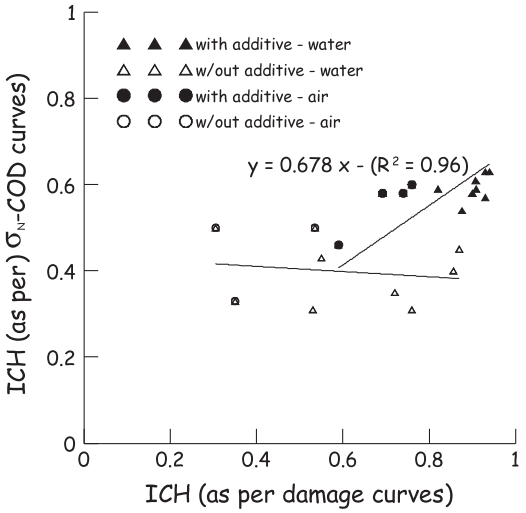

Fig. 17c. Index of crack healing evaluated from σ_N–COD curves vs. damage curves.

with reference to the distance between the units (90 mm, as indicated in the caption of Fig. 4). The velocity, as calculated for each specimen in its virgin state (see above), was assumed as a reference, and denoted as $(UPV)_0$.

The values of the velocities calculated from measured transit times either after pre-cracking or after scheduled exposure/conditioning durations, dimensionless to the aforementioned reference value $(UPV)_0$ have been plotted as a function of the exposure time in Fig. 18 a-c and confirm the statements exposed above with reference to the influence of the crystalline admixture as well as of the exposure conditions on the crack healing.

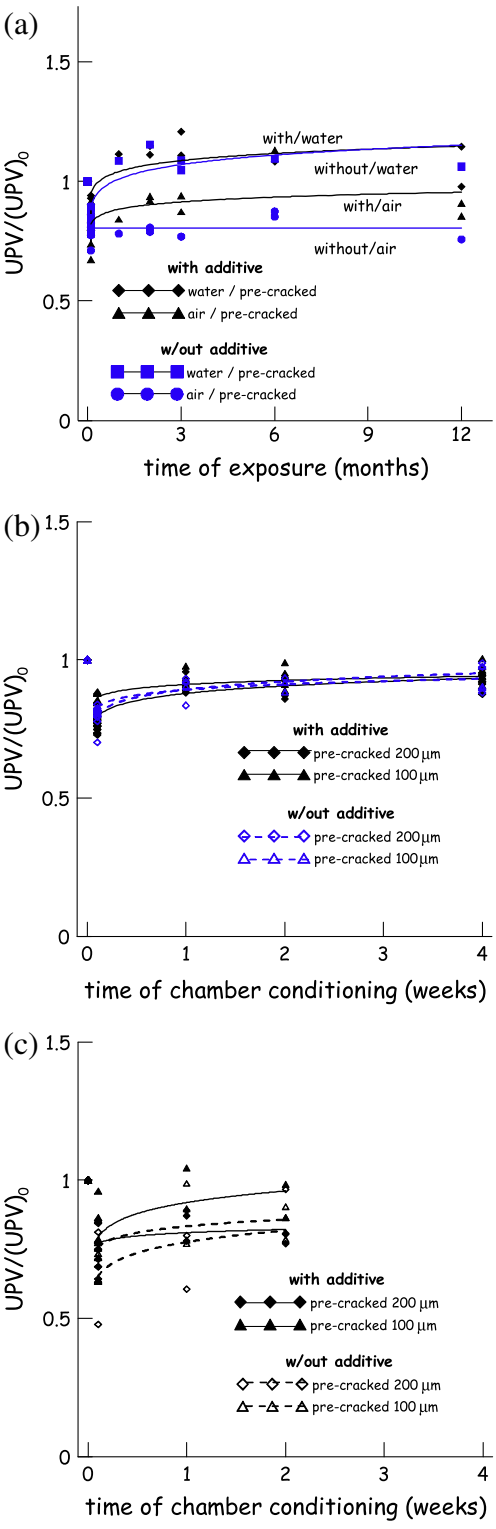

Fig. 18. (a–c) Relative Young moduli vs. exposure time for water immersion and air exposure (a), summer (b) and winter (c) chamber conditioning.

4. SEM analyses

SEM analyses were carried out, at the end of the failure tests performed after the conditioning exposure, on fragments collected from crack surfaces of two concrete specimens, respectively with and without crystalline admixture, after 3 months of immersion in water. Before the conditioning period in water the beam specimen were pre-cracked to a crack opening of 200 µm. The SEM observations were carried out at the end of conditioning period (Figs. 19–23) on the pre-crack surface and on a fresh fracture surface.

The cement matrix of the crack surface is covered with very fine fibrous products (Fig. 19). The morphology of these products is compatible with the crystalline structure of typical self healing products; several authors have documented similar fibrous products [38] which were identified as very common microstructures

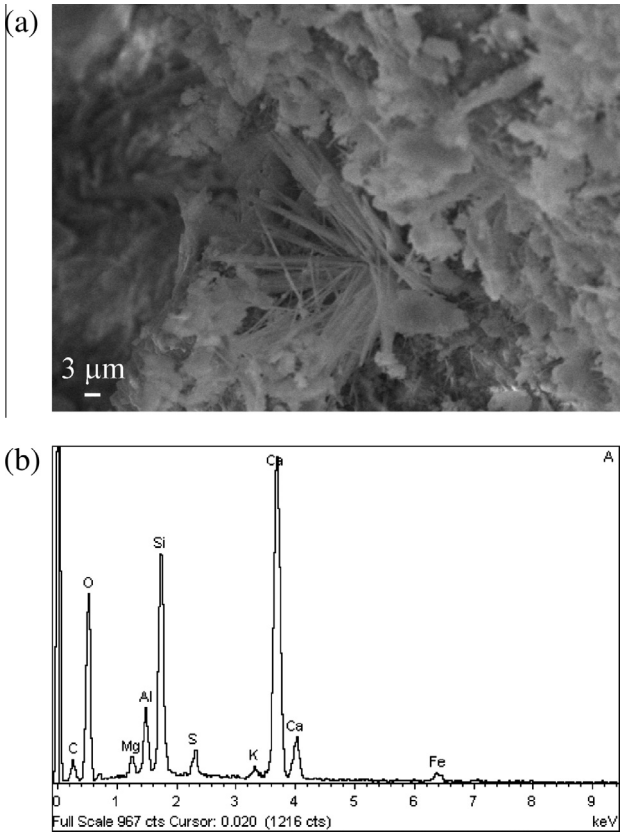

Fig. 19. SEM image (a) and EDS analysis (b) of a sample of concrete specimen with crystalline additive immersed in water for 3 months along the surface parallel to the crack.

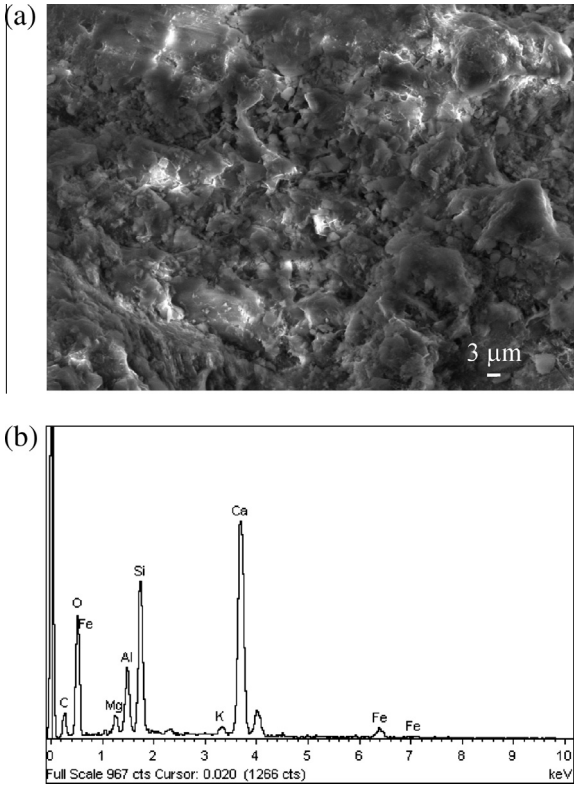

Fig. 20. SEM image (a) and EDS analysis (b) of a sample of concrete specimen with crystalline additive immersed in water for 3 months along the surface orthogonal to the crack.

found in self healed samples. EDS analysis of the products in Fig. 19 shows mainly the typical elements of hydration products of cement (calcium, oxygen and silicon in major amounts, in addition to magnesium, aluminium and potassium); a high peak of sulphur is also present. This is coherent with the composition of the admixture, as shown in Fig. 2. The EDS analysis of the bulk cement paste (not reported here) did not show significant differences with that of fibrous products in Fig. 19; this suggests that in spite of the different morphology of cement paste, the reaction products on crack surface are the result of the growth of same type of fibrous products within the crack. This observation is also in agreement with the macroscopic images of Fig. 14 which show the filling of the crack after the self healing process. The growth of the fibrous products cannot be attributed to the carbonation reaction because of the saturated conditions of slab samples; in fact, diffusion of carbon dioxide is negligible through concrete pores filled with water. Moreover, the time elapsed between the extraction of the specimen from water and the analysis was surely too short to provide any significant precipitation of $CaCO_3$ along the crack surface. Conversely the reaction products should be attributed to hydration reactions involving the crystalline admixture, which were promoted by the water saturated conditions. The morphology of these products and their relative EDS analysis (Fig. 19) also suggest that some ettringite may be present. This matches with findings by Sisomphon and Copuroglu [35], who studied self healing induced by calcium sulfo-aluminate based agents and showed that, upon the ingress of water into the cracks, some ettringite crystals may form inside and fill the same cracks.

These reaction products anyway were not present in the bulk of the concrete which was observed on a fresh fracture surface of the same sample. At the same magnification, it can be observed that the surface orthogonal to the crack (Fig. 20a) shows a different

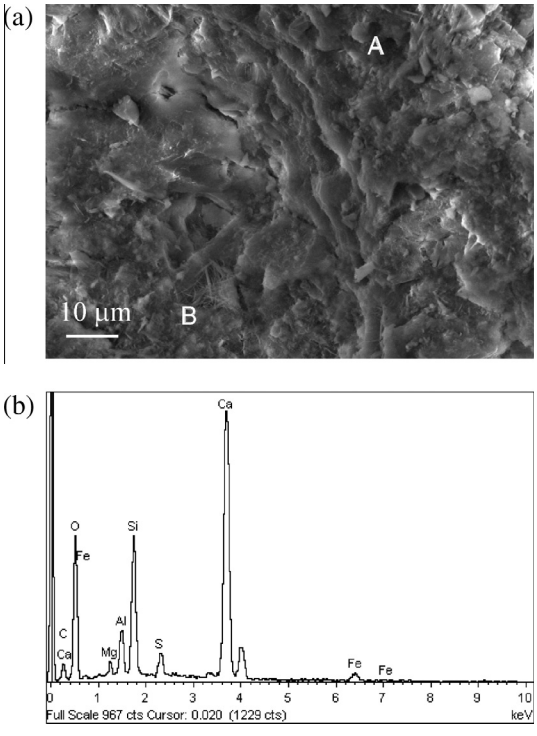

Fig. 21. SEM image (a) and EDS analysis (b) of a sample of concrete specimen with crys talline additive immersed in water for 3 months in correspondence of the area between the crack surface (B) and the one orthogonal to it (A); EDS analysis of zone B (b).

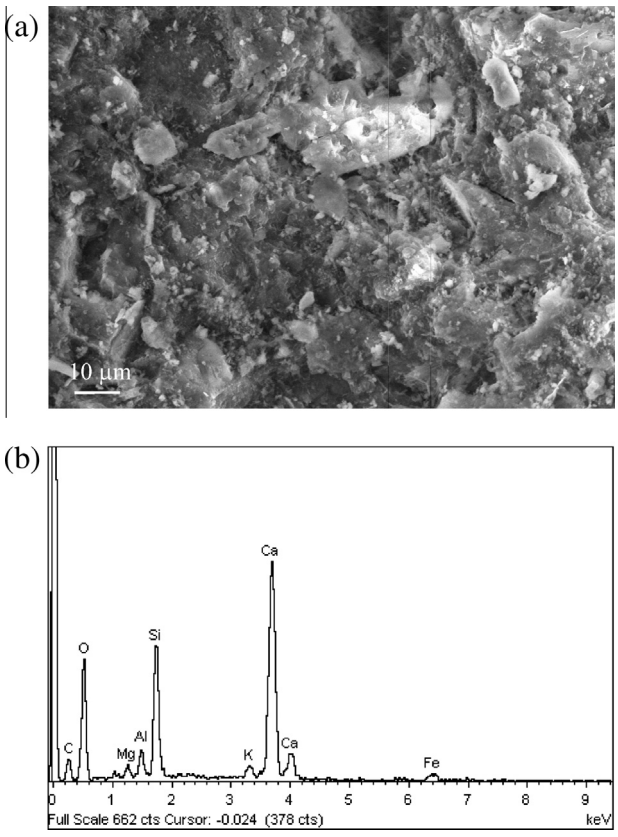

Fig. 22. SEM image (a) and EDS analysis (b) of a sample of concrete specimen without crystalline additive immersed in water for 3 months along the crack surface .

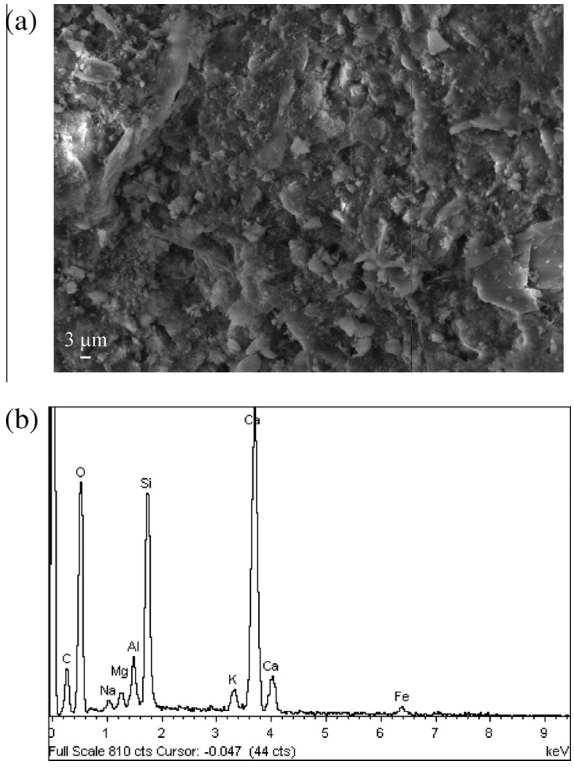

Fig. 23. SEM image (*a*) and EDS analysis (b) of a sample of concrete specimen without crystalline additive immersed in water for 3 months along the crack surface in a zone different from that observed in Fig. 22.

morphology; furthermore, the corresponding EDS analysis (Fig. 20b) differs from that of crack surface (Fig. 19) because of the absence of the peak of sulphur.

The same sample has been observed in correspondence of the area (Fig. 21a) between the crack surface (indicated with the letter B) and the one orthogonal to it (indicated with the letter A); the difference between the area A and B is not morphologically visible but the EDS analysis (Fig. 21b), having made on both zones, confirms the presence of sulphur.

Figs. 22 and 23 show the SEM observations made on a sample collected from a specimen made of concrete without the crystallite additive after 3 months of immersion in water. Figs. 22 and 23 show different zones of the crack surface; it can be observed that the morphology of hydration products is similar to that typical of an ordinary concrete and to the one shown in Fig. 20 (i.e., on the bulk concrete, where the reaction products of the crystalline admixture were not detected). Also EDS analysis carried out on the zone highlighted in Figs. 22 and 23 confirms the absence of the sulphur peak.

5. Conclusions

In this paper a methodology has been proposed and validated to assess and quantify the effects of self healing on the recovery of mechanical properties of normal strength concrete, with and without crystalline admixtures and under different exposure conditions.

The proposed "three-step methodology" includes pre-cracking of specimens, natural or artificially accelerated environmental conditioning under different exposure conditions and, finally, fracture testing of the same specimens up to complete failure. The effects of self healing are assessed and quantified by means of comparison between mechanical behaviour parameters garnered through pre-cracking and failure tests on the same specimen. It is worth once again remarking that the proposed methodology, unlike those based exclusively on the measurement of variations in water permeability, allow the extent and effects of self healing, if any, to be effectively investigated also under exposure conditions other than complete water saturation. Comparative data processing was performed also with the aim of defining self healing indices, in terms of stiffness and load bearing capacity recovery, through which the ratio of crack closure, to the original crack opening, could be inferred.

From the analysed results, the following concluding remarks can be drawn:

- under water immersion even a normal strength concrete inherently possesses some autogenic healing capacity, as witnessed by visual observation (cracks were effectively closed) as well as by the measured recovery of bending stiffness and load bearing capacity, as evaluated through 3-point bending tests; the presence of crystalline additive sped up the crack healing process and related recovery of mechanical properties and furthermore positively affected its final entity;
- in the case of air exposure, even if in quite humid climates, the presence of crystalline additives in the mix design was highly effective in engineering the self healing and the recovery of stiffness and load bearing capacity, in some cases making it quite similar to the case of specimens not containing the additive but immersed in water. In the absence of any self healing catalyst, air exposure was not enough to induce any significant recovery neither of material continuity nor of its mechanical behaviour;
- accelerated exposure conditions, under constant high relative humidity and cycling temperature, may be able to yield results comparable to those obtained under likely favourable natural

exposure conditions; anyway the high dispersion of obtained results does not allow to draw any definitive conclusion. Caution has anyway to be exerted in carefully checking artifacts which may be induced by accelerated temperature cycling, which could counteract and hinder positive effects due to healing phenomena;
- an Index of Load Recovery and an Index of Damage Recovery were defined and calculated from experimental nominal stress and stiffness values, obtained from 3 point bending tests performed on the same specimen in the pre-cracking and in the post-conditioning stage;
- a methodology has been proposed to estimate the ratio of crack closure from comparison between pre-cracking and post-conditioning nominal stress vs. crack opening curves obtained from 3pb tests as well as from damage evolution curves, as built from quantification of the Index of Damage Recovery;
- evolution trends and correlation of the aforementioned stiffness and load recovery vs. crack healing indices showed, that a crack closure above 70–80%, as from graphs in Fig. 17c, is necessary in order to start having an appreciable recovery of stiffness (i.e. larger than 20%); similarly it did occur for load recovery; the presence of the additive made also the evaluated crack healing indices more consistent between each other;
- the same trends detected for bending stiffness and load bearing capacity were also measured for Ultrasonic Pulse Velocity;
- SEM observations and EDS analyses confirmed the presence of reaction products similar to those yielded by cement hydration on the cracked (and thus healed) surfaces. These products were clearly due to the delayed hydration reactions involving the crystalline admixture.

Further validation and extension of the methodology herein proposed would include, e.g., the study of the influence of through-crack stress state, repetition of cracking and healing cycles, and a thorough investigation of Fibre Reinforced Concrete and Cementitious Composites, where the identification of post-cracking residual strength of the material and its degradation/evolution over time, as a function of the exposure conditions, plays a crucial role in the development of a durability based design approach.

Acknowledgements

The authors acknowledge the cooperation of Mrs. Irene Pessina, Silvia Busnelli and Valentina De Monti in performing experimental tests, in partial fulfilment of the requirements for the MEng in Civil Engineering and in Building Engineering. The authors also thank MArch. E. Gastaldo Brac, Penetron Italia, for his support to this research, and acknowledge the financial contribution of Politecnico di Milano, Giovani Ricercatori 2011 grant.

References

[1] Mihashi H, Nishiwaki T. Development of engineered self-healing and self-repairing concrete. State-of-art report. J Adv Concr Technol 2010;10:170–84.
[2] Tittelboom KV, De Belie N. Self-healing in cementitious materials – a review. Materials 2013;6:2182–217.
[3] Lauer KR, Slate FO. Autogeneous healing of cement paste. ACI J 1956;52(6):1083–97.
[4] Bertolini L, Elsener B, Pedeferri P, Polder R. Corrosion of steel in concrete: prevention, diagnosis, repair. Weinheim: Wiley VCH; 2003.
[5] Abrams DA. Tests of bond between concrete and steel. University of Illinois, 1913; Bulletin 71, 107 pp.
[6] Loving MW. Autogenous healing of concrete. American Concrete Pipe Association. 1936, Bullettin 13.
[7] Ramm W, Biscoping M. Autogeneous healing and reinforcement corrosion of water-penetrated separation cracks in reinforced concrete. Nucl Eng Des 1998;179:191–200.
[8] Hearn N, Morley CT. Self-sealing property of concrete: experimental evidence. Mater Struct 1997;30:404–11.
[9] Neville A. Autogenous healing: a concrete miracle? Concr Int 2002;24:76–82.
[10] Turner L. The autogenous healing of cement and concrete: its relation to vibrated concrete and cracked concrete. Intl. Ass. Test. Mats. 1937, London Congress; 344.
[11] Whitehurst EA. Soniscope tests concrete structures. ACI J 1951;47(433–44):4.
[12] Hearn N. Self-sealing, autogenous healing and continued hydration: what is the difference? Mater Struct 1998;31:563–7.
[13] Edvardsen C. Water permeability and autogenous healing of cracks in concrete. ACI Mater J 1999;96:448–54.
[14] Aldea CM, Song WJ, Popovics JS. Extent of healing of cracked normal strength concrete. ASCE J Mater Civ Eng 2000;2:92–6.
[15] Dhir RK, Sangha CM, Munday JG. Strength and deformation properties of autogenously healed mortars. ACI J 1973;70:231–6.
[16] Reinhardt HW, Jooss M. Permeability and self-healing of cracked concrete as a function of temperature and crack width. Cem Concr Res 2003;33:981–5.
[17] Jacobsen S, Sellevold EJ. Self healing of high strength concrete after deterioration by freeze/thaw. Cem Concr Res 1993;26:55–62.
[18] Sahmaran M, Keskin SB, Ozerkan G, Yaman IO. Self healing of mechanically loaded self consolidating concretes with high volumes of fly ash. Cem Concr Compos 2008;30:872–9.
[19] Ngab AS, Nilson AH, Slate FO. Shrinkage and creep of high strength concrete. ACI J 1981;78:225–61.
[20] Hannant DJ, Keer JG. Autogenous healing of thin cement based sheets. Cem Concr Res 1983;13:357–65.
[21] Grey DJ. Autogenous healing of fiber/matrix interfacial bond in fiber reinforced mortar. Cem Concr Res 1984;14:315–7.
[22] Yang Y, Lepech MD, Yang EH, Li VC. Autogenous healing of engineered cementitious composites under wet–dry cycles. Cem Concr Res 2009;39:382–90.
[23] Qian S, Zhou J, de Rooji MR, Schlangen E, Ye G, van Breugel K. Self-healing behavior oif strain hardening cementitious composites incorporating local waste materials. Cem Concr Compos 2009;31:613–21.
[24] Qian SZ, Zhou J, Schlangen E. Influence of curing condition and precracking time on the self-healing behavior of engineered cementitious composites. Cem Concr Compos 2010;32:686–93.
[25] Yang Y, Yang EH, Li VC. Autogeneous healing of engineered cementitious composites at early age. Cem Concr Res 2011;41:176–83.
[26] Li M, Li VC. Cracking and healing of engineered cementititous composites under chloride environment. ACI Mater J 2011;108:333–40.
[27] Ferrara L, Krelani V, Geminiani M, Gorlezza R. Self healing of high performance fibre reinforced cementitious composites. In: Improving performance of concrete structures. Proc. 4th Intl. fib Congress 2014 Mumbai, India, 10-14 February 8 2014, 883–887.
[28] Mihashi H, Ahmed SFU, Kobayakawa A. Corrosion of reinforcing steel in fiber reinforced cementitious composites. J Adv Concr Technol 2011;9:159–67.
[29] Jonkers HM. Bacteria based self-healing concrete. Heron 2010;56(1/2):1–12.
[30] RILEM TC 225-SAP. Application of Superabsorbent Polymers (SAP). In: Mechtcherine V, Reinhardt HW, editors, Concrete construction, state of the art report prepared by technical committee 225-SAP, Springer, 2012, X, 166 p.
[31] Van Tittelboom K, De Belie N, Van Loo D, Jacobs P. Self-healing efficiency of cementitious matgerials containing tubular capsules filled with healing agent. Cem Concr Compos 2011;33:497–505.
[32] Yang Z, Hollar J, He X, Shi X. A self-healing cementitious composite using oil/core silica gel shell microcapsules. Cem Concr Compos 2011;33:506–12.
[33] ACI 212-3R-10. Report on chemical admixtures for concrete. 2010, 61pp.
[34] Termkhajornkit P, Nawa T, Yamashiro Y, Saito T. Self healing ability of fly ash-cement systems. Cem Concr Compos 2009;31:195–203.
[35] Sisomphon K, Copuroglu O. Self healing mortars by using different cementitious materials. In: Proc. Intl. Conf. on Advances in construction materials through science and engineering, Hong Kong, China, 5-7 September 2011.
[36] Carsana M, Frassoni M, Bertolini L. Comparison of ground-waste-glass with other supplementary cementitious materials. Cem Concr Compos 2014;45:39–45.
[37] Bertolini L, Carsana M, Frassoni M, Gelli M. Pozzolanic additions for durability of concrete structures. Constr Mater ICE 2011;164:283–91.
[38] Gagné R, Argouges M. A study of the natural self-healing of mortars using air-flow measurements. Mater Struct 2012;45:1625–38.